



Rapid Determination of Fast Protein Dynamics from NMR Chemical Exchange Saturation Transfer Data

Yina Gu, Alexandar L. Hansen, Yu Peng, and Rafael Brüschweiler*

Abstract: Functional motions of ^{15}N -labeled proteins can be monitored by solution NMR spin relaxation experiments over a broad range of timescales. These experiments however typically take of the order of several days to a week per protein. Recently, NMR chemical exchange saturation transfer (CEST) experiments have emerged to probe slow millisecond motions complementing $R_{1\rho}$ and CPMG-type experiments. CEST also simultaneously reports on site-specific R_1 and R_2 parameters. It is shown here how CEST-derived R_1 and R_2 relaxation parameters can be measured within a few hours at an accuracy comparable to traditional relaxation experiments. Using a “lean” version of the model-free approach S^2 order parameters can be determined that match those from the standard model-free approach applied to ^{15}N R_1 , R_2 , and $\{^1\text{H}\}$ - ^{15}N NOE data. The new methodology, which is demonstrated for ubiquitin and arginine kinase (42 kDa), should serve as an effective screening tool of protein dynamics from picosecond-to-millisecond timescales.

The recent emergence of CEST^[1] and dark-state exchange saturation transfer (DEST) experiments^[2] permits the sensitive detection of lowly populated, slowly interconverting conformational substates of proteins, thereby complementing well-established $R_{1\rho}$ ^[3] and CPMG experiments.^[4] CEST reports on the presence of such “excited” protein states indirectly by measuring the signal of a ground-state resonance in the presence of a variable-offset radio-frequency (rf) B_1 saturation field. When the B_1 field is applied at the frequency of the excited state resonance, saturation is transferred to the ground state by the exchange process(es), which is manifested as a dip in the CEST intensity profile from which kinetic rates ($k_{\text{ab}} + k_{\text{ba}} = k_{\text{ex}}$) together with the population of the excited state (p_{b}) and its chemical shift can be extracted. In addition to these slow exchange processes, CEST profiles also reflect longitudinal R_1 and transverse R_2 relaxation rates of the

protein ground state, providing a potentially alternative source of these parameters for quantitative studies of nano- and picosecond dynamics. These parameters do not only characterize dynamic loop regions, which are often involved in protein–protein interfaces,^[5] but they also represent unique reporters of the conformational entropy at atomic resolution providing unique insights into this driving force of molecular function.^[6] However, it is unclear whether CEST-derived ^{15}N R_1 and R_2 values can be determined as accurately and precisely as those obtained from traditional relaxation experiments, which has important consequences for their interpretation in terms of protein dynamics.

Information about fast timescale dynamics can be extracted from ^{15}N R_1 , R_2 and $\{^1\text{H}\}$ - ^{15}N NOE data by the model-free approach (MFA)^[7] with various software packages available.^[8] The general goal of MFA is to extract a S^2 order parameter for each ^{15}N site, which is a measure for the motional restriction of the N–H bond vector in the molecular frame, along with an internal motional correlation time τ_{int} . Extended variants of the model-free analysis exist,^[9] but in practice the extended model-free approach is often equivalent to MFA.^[10]

Here, we explore the exclusive use of CEST-derived R_1 , R_2 data for their interpretation by MFA. Since CEST does not report about the $\{^1\text{H}\}$ - ^{15}N NOE, and by avoiding a separate NOE experiment because of its time-consuming nature, R_1 , R_2 are interpreted by a lean version of the model-free approach, referred to as L-MFA. The performance of L-MFA is rigorously tested by comparison with MFA using simulated relaxation parameter sets derived from ten extended protein molecular dynamics simulations. With CEST-derived relaxation rates serving as input for L-MFA fitting to extract S^2 order parameters, an integrated protocol is established that aims at the rapid characterization of protein dynamics on the picosecond to nanosecond timescale, while simultaneously gaining insight into millisecond motions, solely based on a single CEST profile.

To assess the quality of CEST-derived relaxation parameters, R_1 , R_2 data from CEST were compared with R_1 , R_2 data obtained from standard spin relaxation experiments all measured at 850 MHz magnetic field strength. Figure 1 shows that the data obtained for ubiquitin are in remarkably good agreement with each other with Pearson correlation coefficients of 0.97 and 0.98 and root-mean-square (RMS) errors of 0.03 (ca. 2 %) and 0.40 (ca. 5 %) for R_1 and R_2 , respectively. The large R_2 rates for residues I23, N25 are consistent with values reported previously for these residues as they undergo dynamic exchange.^[11] Similarly good agreement between CEST-derived and traditionally measured R_1 , R_2 parameters were obtained for a protein of substantially larger size, which is the apo state of the 42 kDa arginine kinase (AK, see Figure S1 in the Supporting Information).

[*] Y. Gu, Dr. Y. Peng, Prof. Dr. R. Brüschweiler
Department of Chemistry and Biochemistry
The Ohio State University
100 West 18th Avenue, Columbus, OH 43210 (USA)
E-mail: bruschweiler.1@osu.edu

Dr. A. L. Hansen, Prof. Dr. R. Brüschweiler
Campus Chemical Instrument Center
The Ohio State University
460 W. 12th Avenue, Columbus, OH 43210 (USA)
Prof. Dr. R. Brüschweiler
Department of Biological Chemistry and Pharmacology, The Ohio State University
1645 Neil Avenue, Columbus, OH 43210 (USA)

Supporting information for this article is available on the WWW under <http://dx.doi.org/10.1002/ange.201511711>.

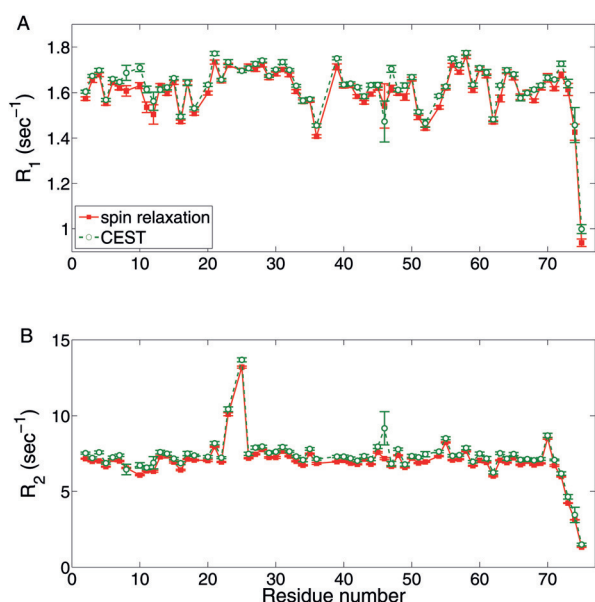


Figure 1. Comparison of experimental relaxation parameters A) R_1 and B) R_2 of ubiquitin derived from CEST (green circles) and standard spin relaxation experiments (red squares) at 850 MHz magnetic field strength. Residue T9 is not shown because of substantial broadening of this peak at pH 7 resulting in a large uncertainty of its relaxation parameters.

When performing CEST experiments, the choice of the strength of the B_1 saturating field is important. With larger B_1 fields, greater step sizes can be used for the frequency sweep and, hence, fewer B_1 points need to be measured, which shortens the duration of the experiment. However, larger B_1 fields lead to broadened CEST profiles resulting in lower resolution and lower sensitivity to the presence of exchange processes. If only a single field is to be used, we find that $\gamma B_1 / 2\pi = 100$ Hz represents a good compromise. It can be optionally paired with a second B_1 field at 25 Hz to more accurately characterize residues experiencing chemical exchange,^[12] which is discussed in greater detail in the Supporting Information.

Before analyzing experimental CEST-derived relaxation parameters by L-MFA, we tested the accuracy and stability of the L-MFA approach for the determination of S^2 solely based on ^{15}N R_1 and R_2 relaxation rates. For this purpose, we compared the S^2 values computed by L-MFA and MFA for ten proteins fitted from relaxation parameters derived from 500 ns molecular dynamics (MD) trajectories (see the Supporting Information). We find that discarding the heteronuclear $\{^1\text{H}\}$ - ^{15}N NOEs has only minimal effect on the S^2 values. For example, the S^2 profiles of the ATPase α -domain (PDB: 1QZM) determined by the two model-free methods are nearly identical (Figure 2 inset). The correlation coefficient between $S^2_{\text{L-MFA}}$ and S^2_{MFA} is 1.00 and the RMS error is 0.012. The optimal overall tumbling correlation time τ_c value estimated from R_2/R_1 ratios is 9.87 ns compared to the true value of 10.00 ns. This leads to a small, systematic offset of $S^2_{\text{L-MFA}}$ toward larger values compared to S^2_{MFA} . Further analyses were performed for proteins of different sizes represented by different tumbling correlation times τ_c of 5, 10, and 15 ns (Figures S3–S12).^[13] Isotropic diffusion was chosen for L-MFA as it applies in very good approximation for globular

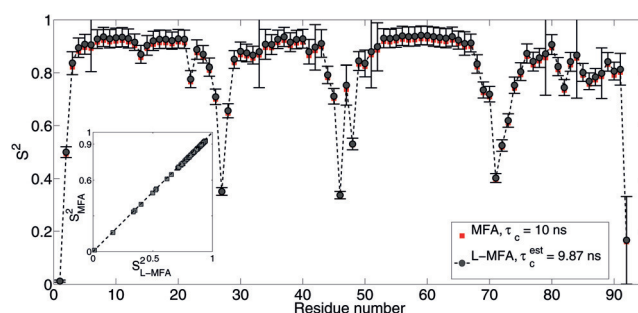


Figure 2. Comparison of backbone N–H S^2 order parameters obtained by L-MFA and MFA model-free analysis of the α -domain of ATPase (PDB 1QZM) based on NMR spin relaxation data computed from a 500 ns MD trajectory assuming a tumbling correlation time $\tau_c = 10$ ns. An estimated $\tau_c = 9.87$ ns based on the average R_2/R_1 ratio of residues in well-defined secondary structures was used for the L-MFA analysis. The inset shows a correlation plot of S^2_{MFA} versus $S^2_{\text{L-MFA}}$ with different τ_c values of 10 and 9.87 ns, respectively. The correlation coefficient between S^2_{MFA} and $S^2_{\text{L-MFA}}$ is 1.00 and the RMS error is 0.012.

proteins and does not require a high-resolution 3D protein structure. While for some of the most mobile residues the uncertainties in S^2 , estimated from 30 Monte Carlo simulations assuming 5% errors for R_1 and R_2 , tend to increase, for all systems studied here, the S^2 profiles extracted by the two model-free analysis methods (L-MFA and MFA) show a very high level of consistency.

After having been validated by simulations, the L-MFA method was applied to the experimental CEST-derived ^{15}N relaxation parameters for ubiquitin and arginine kinase. In general, S^2 values from L-MFA of CEST-derived R_1 , R_2 rates closely match the results from MFA applied to a full set of spin relaxation parameters (Figure 3). For ubiquitin, a high correlation coefficient ($R = 0.97$) and a small error (RMS = 0.03) between $S^2_{\text{L-MFA}}$ and S^2_{MFA} demonstrates the ability to derive accurate S^2 values directly from CEST experiments. Good agreement is also found between $S^2_{\text{L-MFA}}$ and the previously published S^2 profile for protein arginine kinase (see Figure S2).^[14] In particular, there is excellent agreement in the V308–V322 loop near the C-terminus, which is by far the most dynamic region of AK on the ps–ns timescale by displaying a consistently low S^2 around 0.4 for both sets of

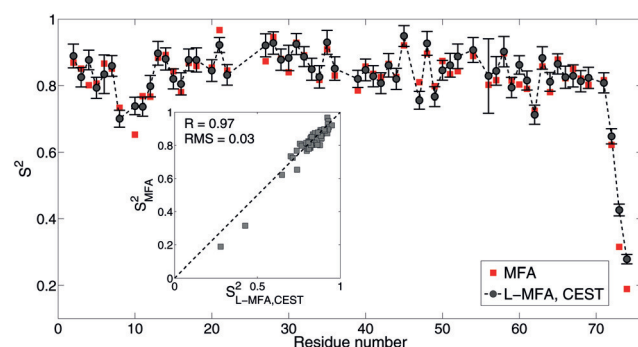


Figure 3. Comparison of experimental ubiquitin order parameters S^2_{MFA} determined from R_1 , R_2 and NOE data of standard spin relaxation experiments (red squares) and $S^2_{\text{L-MFA}}$ determined from CEST-derived R_1 , R_2 values (black circles). The inset shows a scatter plot of the two types of order parameters.

experiments. In addition, we evaluated the accuracy with which internal correlation times τ_{int} could be extracted by the L-MFA method and found that, while the L-MFA-derived τ_{int} values agree quite well with MFA results for ubiquitin (Figure S14), the overall uncertainty in τ_{int} is larger. This is because unlike S^2 values, typical sub-ns τ_{int} values are particularly sensitive to the heteronuclear $\{^1\text{H}\}\text{-}^{15}\text{N}$ NOE, which L-MFA does not use.

In summary, our results show that CEST permits the extraction of R_1 and R_2 relaxation parameters that are equivalent to those determined by traditional methods and they can be analyzed via the L-MFA method for the reliable determination of S^2 order parameter profiles. A speed up can also be achieved with traditional NMR relaxation experiments by discarding the heteronuclear NOE experiment and recording R_1 and R_2 only, followed by L-MFA analysis. However, in this case one would not gain insights into the slow exchange dynamics that CEST offers in addition. Moreover, when exchange is observed in the CEST profile, accurate ground-state R_1 and R_2 values can be obtained by fitting the exchange contribution (see the Supporting Information), whereas this contribution would merely be averaged into the rates determined from traditional spin relaxation experiments. For the proteins studied in this work, the agreement between CEST-derived and traditionally measured R_1 , R_2 relaxation parameters is remarkable considering the highly complementary nature of the two approaches: CEST extracts relaxation information from partially saturated resonances at variable off-resonance frequencies, whereas the traditional method measures exponential magnetization decays. The CEST-based strategy proposed here is promising for efficient routine screening of proteins of dynamics properties and their changes that might be of functional relevance, such as free versus complexed or wild-type versus mutant protein states.

Experimental Section

NMR experiments were carried out at 800 MHz (apo-AK) or 850 MHz (ubiquitin) on Avance III HD Bruker instruments equipped with TXI (800) or TCI (850) cryoprobes. ^{15}N CEST experiments were performed using the experiments of Vallurupalli et al.^[1c] with B_1 field strengths of 30 and 60 Hz, for apo-AK, and 25 and 100 Hz for ubiquitin. The B_1 field was swept from 90 to 150 ppm in each of the CEST experiments and acquired in 6 hours (ubiquitin with 100 Hz field) and 39 hours (apo-AK with 30 Hz field). All CEST data was processed with the nmrPipe^[15] and intensity profiles analyzed using ChemEx^[1c] (<http://www.github.com/gbouvignies/chemex>). ^{15}N spin relaxation experiments were performed on ubiquitin at 850 MHz using HSQC-based experiments^[16] with a minor modification for fully protonated samples.^[17] The combined acquisition time for R_1 and R_2 experiments of ubiquitin was eight hours. Detailed experimental setups and analyses of all experiments can be found in the Supporting Information.

Acknowledgements

This work was supported by the National Science Foundation (grant number MCB-1360966) and the NIH (grant number 5R01GM077643). All CEST experiments were performed at the CCIC NMR facility at OSU.

Keywords: CEST · lean model-free analysis · NMR spectroscopy · protein dynamics · spin relaxation

How to cite: *Angew. Chem. Int. Ed.* **2016**, *55*, 3117–3119
Angew. Chem. **2016**, *128*, 3169–3171

- [1] a) G. Bouvignies, L. E. Kay, *J. Phys. Chem. B* **2012**, *116*, 14311–14317; b) G. Bouvignies, L. E. Kay, *J. Biomol. NMR* **2012**, *53*, 303–310; c) P. Vallurupalli, G. Bouvignies, L. E. Kay, *J. Am. Chem. Soc.* **2012**, *134*, 8148–8161; d) B. Zhao, A. L. Hansen, Q. Zhang, *J. Am. Chem. Soc.* **2014**, *136*, 20–23.
- [2] a) N. L. Fawzi, J. F. Ying, R. Ghirlando, D. A. Torchia, G. M. Clore, *Nature* **2011**, *480*, 268–U161; b) N. L. Fawzi, J. F. Ying, D. A. Torchia, G. M. Clore, *Nat. Protoc.* **2012**, *7*, 1523–1533; c) D. S. Libich, N. L. Fawzi, J. F. Ying, G. M. Clore, *Proc. Natl. Acad. Sci. USA* **2013**, *110*, 11361–11366; d) N. L. Fawzi, D. S. Libich, J. F. Ying, V. Tugarinov, G. M. Clore, *Angew. Chem. Int. Ed.* **2014**, *53*, 10345–10349; *Angew. Chem.* **2014**, *126*, 10513–10517.
- [3] a) A. G. Palmer 3rd, C. D. Kroenke, J. P. Loria, *Methods Enzymol.* **2001**, *339*, 204–238; b) A. Mittermaier, L. E. Kay, *Science* **2006**, *312*, 224–228; c) A. G. Palmer 3rd, F. Massi, *Chem. Rev.* **2006**, *106*, 1700–1719; d) D. M. Korzhnev, L. E. Kay, *Acc. Chem. Res.* **2008**, *41*, 442–451.
- [4] a) H. Y. Carr, E. M. Purcell, *Phys. Rev.* **1954**, *94*, 630–638; b) S. Meiboom, D. Gill, *Rev. Sci. Instrum.* **1958**, *29*, 688–691; c) A. C. Sauerwein, D. F. Hansen, in *Protein NMR*, Vol. 32 (Ed.: L. Berliner), Springer, US, **2015**, pp. 75–132.
- [5] Y. Gu, D. W. Li, R. Brüschweiler, *J. Chem. Theory Comput.* **2015**, *11*, 1308–1314.
- [6] a) M. Akke, R. Brüschweiler, A. G. Palmer 3rd, *J. Am. Chem. Soc.* **1993**, *115*, 9832–9833; b) D. Yang, L. E. Kay, *J. Mol. Biol.* **1996**, *263*, 369–382; c) Z. Li, S. Raychaudhuri, A. J. Wand, *Protein Sci.* **1996**, *5*, 2647–2650.
- [7] a) G. Lipari, A. Szabo, *J. Am. Chem. Soc.* **1982**, *104*, 4559–4570; b) G. Lipari, A. Szabo, *J. Am. Chem. Soc.* **1982**, *104*, 4546–4559.
- [8] a) A. M. Mandel, M. Akke, A. G. Palmer 3rd, *J. Mol. Biol.* **1995**, *246*, 144–163; b) P. Dosset, J. C. Hus, M. Blackledge, D. Marion, *J. Biomol. NMR* **2000**, *16*, 23–28; c) R. Cole, J. P. Loria, *J. Biomol. NMR* **2003**, *26*, 203–213; d) M. Bieri, E. J. O’Auvergne, P. R. Gooley, *J. Biomol. NMR* **2011**, *50*, 147–155.
- [9] G. M. Clore, A. Szabo, A. Bax, L. E. Kay, P. C. Driscoll, A. M. Gronenborn, *J. Am. Chem. Soc.* **1990**, *112*, 4989–4991.
- [10] L. Jaremko, M. Jaremko, M. Nowakowski, A. Ejchart, *J. Phys. Chem. B* **2015**, *119*, 11978–11987.
- [11] a) N. Tjandra, S. E. Feller, R. W. Pastor, A. Bax, *J. Am. Chem. Soc.* **1995**, *117*, 12562–12566; b) S. F. Lienin, T. Bremi, B. Brutscher, R. Brüschweiler, R. R. Ernst, *J. Am. Chem. Soc.* **1998**, *120*, 9870–9879.
- [12] a) A. L. Hansen, G. Bouvignies, L. E. Kay, *J. Biomol. NMR* **2013**, *55*, 279–289; b) M. G. Carneiro, J. G. Reddy, C. Griesinger, D. Lee, *J. Biomol. NMR* **2015**, *63*, 237–244.
- [13] Y. Gu, D. W. Li, R. Brüschweiler, *J. Chem. Theory Comput.* **2014**, *10*, 2599–2607.
- [14] O. Davulcu, P. F. Flynn, M. S. Chapman, J. J. Skalicky, *Structure* **2009**, *17*, 1356–1367.
- [15] F. Delaglio, S. Grzesiek, G. W. Vuister, G. Zhu, J. Pfeifer, A. Bax, *J. Biomol. NMR* **1995**, *6*, 277–293.
- [16] N. A. Lakomek, J. Ying, A. Bax, *J. Biomol. NMR* **2012**, *53*, 209–221.
- [17] M. Gairí, A. Dyachenko, M. T. Gonzalez, M. Feliz, M. Pons, E. Giralt, *J. Biomol. NMR* **2015**, *62*, 209–220.

Received: December 17, 2015

Published online: January 28, 2016